ORNL/TR--90/28

DE91 008916

INVESTIGATION OF 1-cm DOSE EQUIVALENT FOR PHOTONS BEHIND SHIELDING MATERIALS

Hideo Hirayama
National Laboratory for High Energy Physics
Oho, Tsukuba-shi, Ibaraki-ken, 305, Japan
and
Shun-ichi Tanaka
Japan Atomic Research Institute
Tokai-mura, Ibaraki-ken, 319-11, Japan

DATE PUBLISHED: March 1991

Prepared by the
OAK RIDGE NATIONAL LABORATORY
Oak Ridge, Tennessee 37831
managed by
MARTIN MARIETTA ENERGY SYSTEMS, INC.
for the
U.S. DEPARTMENT OF ENERGY
under contract No. DE-AC05-84OR21400

PREFACE

Newly available standard reference data, "Neutron and Gamma-Ray Fluence-to-Dose Factors," ANSI/ANS-6.1.1-1990 and "Gamma-Ray Attenuation Coefficients and Buildup Factors for Engineering Materials," ANSI/ANS-6.4.3-1990, are of great value for engineering shield design. The first document gives guidance in the use of radiation spectra to calculate dose for radiation protection purposes. The second document gives gamma-ray transport data for various source energies, but not for spectra emerging from shields. Therefore, the data from the first cannot logically be applied to point kernel calculations based on the second. Furthermore, the buildup factors give exposure in an infinite medium, not dose equivalent for a finite shield as is needed for radiation protection applications.

Tanaka *et al* have solved these problems and prescribed the method to be used in compliance with the new Japanese radiological protection law. The method and the underlying research were published in Japanese. We felt that the work should be made available to a wider audience, and so we asked the authors to translate the publications into English which we are making available as Oak Ridge National Laboratory reports.[1]

Hirayama and Tanaka in the first report describe the theory and research which provide "average" and "practical" conversion factors to compute ambient (1-cm) dose equivalent for finite and infinite shields. These can be applied as correction factors to computed exposure. A significant aspect of these calculations is the effect of charged particles in the assumed 10-cm-thick air gap behind the shield.

Tanaka and Suzuki in the second report provide the "effective conversion factors" for 1-cm, 3-mm, and 70-μm depth dose equivalent to convert from absorbed dose in air. Tables to correct to a finite shield are also given. The report provides guidance for the inexperienced and includes a detailed step-by-step example for a practical shielding calculation.

The ANS-6.4.3 standard also provides correction factors to take into account the energy deposition in a phantom following the shield. These corrections, however, provide the maximum dose in the phantom, rather than at prescribed depths. For that reason, mainly, we recommend the Tanaka correction factors instead.

The present technology is implemented in the computer code systems QAD-CGGP2 and G33-GP2.

D. K. Trubey
Chairman, ANS-6 and ANS-6.4.3
Radiation Shielding Information Center

November 1990

---

[1]ORNL/TR-90/28 and ORNL/TR-90/29.

Investigation of 1 cm Dose Equivalent for Photons behind Shielding Materials*

HIDEO HIRAYAMA

National Laboratory for High Energy Physics
Oho, Tsukuba-shi, Ibaraki-ken, 305, Japan

and

SHUN-ICHI TANAKA

Japan Atomic Research Institute, Tokai-mura, Ibaraki-ken, 319-11 Japan

ABSTRACT

The ambient dose equivalent at 1-cm depth, assumed equivalent to the 1-cm dose equivalent in practical dose estimations behind shielding slabs of water, concrete, iron or lead for normally incident photons having various energies was calculated by using conversion factors for a slab phantom. It was compared with the 1-cm depth dose calculated with the Monte Carlo code EGS4. It was concluded from this comparison that the ambient dose equivalent calculated by using the conversion factors for the ICRU sphere could be used for the evaluation of the 1-cm dose equivalent for the sphere phantom within 20 % errors.

Average and practical conversion factors are defined as the conversion factors from exposure to ambient dose equivalent in a finite slab or an infinite one, respectively. They were calculated with EGS4 and the discrete ordinates code PALLAS. The exposure calculated with simple estimation procedures such as point kernel methods can be easily converted to ambient dose equivalent by using these conversion factors. The maximum value between 1 and 30 mfp can be adopted as the conversion factor which depends only on material and incident photon energy. This gives the ambient dose equivalent on the safe side.

---

* Translation of J. At. Energy Soc. Japan, 31, 101-111 (1989) by the authors.

1. Introduction

It was decided that the 1-cm dose equivalent [$H(10)$], which is the dose equivalent at 1-cm depth of ICRU sphere, is to be used as the effective dose equivalent for external exposure with the revised radiological protection law. $H(10)$ is the practical dose introduced in place of the unmeasurable effective dose equivalent because it is similar to the effective dose equivalent. Moreover, it was also decided that $H(10)$ in the practical field is equivalent to the ambient dose equivalent ($H^*(10)$). $H^*(10)$ can be calculated from the photon flux with the 1-cm dose equivalent conversion factor. Outlines of the revised regulation and the technical problems related to the revision were explained in this journal (*J. of the Atomic Energy Society of Japan*)[1][2]

However, the discussions concerning $H(10)$ were limited to that in free space. $H(10)$ in complicated fields like those behind a shield has not been studied yet. $H(10)$ is calculated from the absorbed dose at 1-cm depth of the human body by modifying with the quality factor and correction factor (both factors are 1 in the case of photons). $H^*(10)$ in free space is always larger than $H(10)$ as mentioned in the previous paper[1][2]. However, this relation is not obvious at the surface of the human body behind the shield due to the fact that charged particle equilibrium is not established in general. It is important to study the relation between $H^*(10)$ and $H(10)$ in various situations. Moreover, it is difficult to apply the energy-dependent 1-cm dose equivalent conversion factor to point kernel calculations which are widely used in shielding designs for photons. The investigations as to how to evaluate $H^*(10)$ in practical shield designs are also very important.

In this study, we examine the relation between the absorbed dose of the slab phantom behind the shield and $H^*(10)$ by using the electron-gamma shower Monte Carlo code EGS4[3]. The applicability of the average conversion factors and practical conversion factors calculated with EGS4 and the discrete ordinates code PALLAS[4] was investigated as the practical method to evaluate $H^*(10)$ in point kernel calculations.

2. Absorbed Dose in A Phantom Behind a Shield

Radiation fields behind a shield are complex fields consisting of photons, electrons and positrons in a distribution spreading in both energy and direction even in the case of normally incident monoenergetic photons on the shield. The 1-cm dose equivalent conversion factors adopted in the revised regulation have been calculated for the ICRU sphere phantom. However, the spherical phantom is a very complex geometry for the calculation of the absorbed dose inside the phantom behind the shield. We did the comparisons, therefore, for the slab phantom among $H(10)$ calculated from the absorbed dose inside the phantom, $H^*(10)$ calculated by using 1-cm dose equivalent conversion factors for a slab phantom, and the maximum dose equivalent obtained from the maximum dose equivalent conversion factors. The latter give the maximum dose equivalent inside the phantom. The electron-gamma shower Monte Carlo code, EGS4, was used for the calculation of the absorbed dose in the field where the charged particle equilibrium does not exist.

2.1. 1-CM DOSE EQUIVALENT AND MAXIMUM DOSE EQUIVALENT CONVERSION FACTORS FOR SLAB PHANTOM

The 1-cm dose equivalent and maximum dose equivalent conversion factors for normally incident plane-parallel photon beams on the semi-infinite slab phantom 30-cm thick calculated by Rogers[5] with EGS3 are used in the following discussion and are shown in Figure 1. The 1-cm dose equivalent conversion factors for the ICRU sphere, which were adopted in ICRP-51[5] and the revised regulation, are also shown in Figure 1 for comparison. Both conversion factors calculated by Rogers were obtained for a 30-cm-thick slab phantom of ICRU soft tissue equivalent phantom in a vacuum. On the other hand, those for the ICRU sphere were average values of the kerma approximation[6] depending on the assumption that charged particle equilibrium exists, and the calculations[7] in vacuum added the contributions of secondary electrons created by the interaction with air.

The 1-cm dose equivalent conversion factors for a slab phantom are slightly larger than those for the ICRU sphere below 3 MeV. This tendency is due to the fact that the contribution of scattered radiations is larger for plane geometry than for a spherical one. Above 3 MeV, those for the ICRU sphere (assuming charged particle equilibrium), become larger than those for the slab phantom (neglecting secondary electrons created in air), and are almost the same as the maximum dose equivalent conversion factors for plane geometry. The reason that the maximum dose equivalent conversion factors are larger than the 1-cm dose equivalent conversion factors for plane geometry in this energy region can

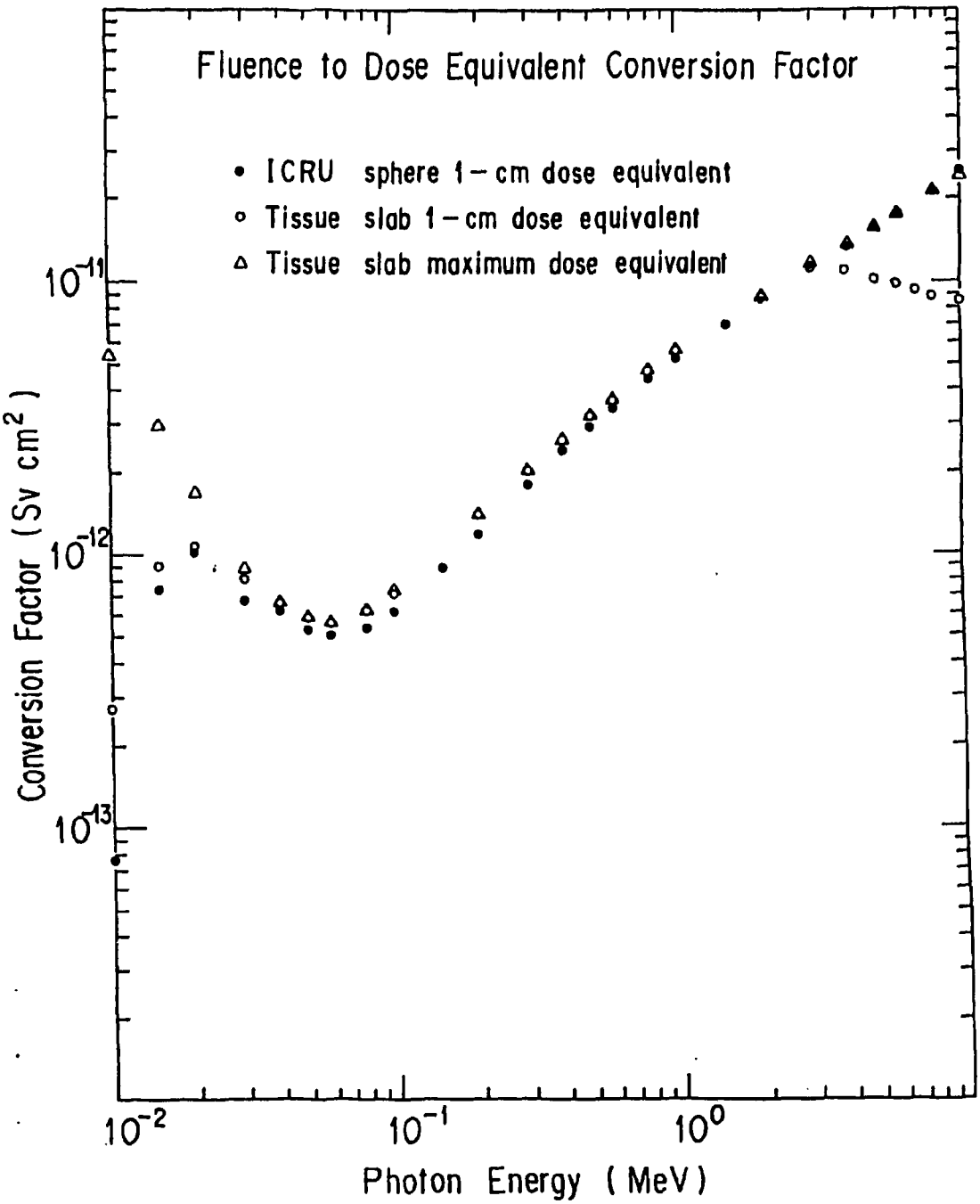

Fig. 1 Fluence to 1-cm dose equivalent conversion factor for both 30 cm-thick slab[5] and 30 cm-diameter phantoms[13] , and fluence to maximum dose equivalent conversion factor for a slab phantom.[5]

be explained from the fact that the position of the maximum absorbed dose moves to deep inside the phantom with an increase of photon energy. At the higher photon energies, one cannot be certain that the absorbed energy in a 30-cm-diameter sphere phantom is equal to that calculated by using kerma, i.e., charged particle equilibrium exists.[9] For example, a distance of 40 m from the injection point is required for charged particle equilibrium to be established in air for 10-MeV photons in a parallel beam of 5-cm radius. Therefore, it can be concluded that the conversion factors for the ICRU sphere, which assumes charged particle equilibrium, give the upper limit of $H(10)$ for the sphere phantom in a practical field.

The maximum dose equivalent conversion factors become larger than both 1-cm dose equivalent conversion factors below 30 keV. In this energy region, incident photons are almost entirely absorbed at the surface of the phantom and the number of photons penetrating to 1-cm depth decreases drastically.

2.2. Radiation Fields and Absorbed Dose in Slab Phantom behind Shields

As examples of radiation fields behind shields, the energy spectra of photons , electrons and positrons (charged particles) and the absorbed dose in a 30 cm-thick water phantom following a 10-cm air region were calculated by EGS4 behind water, concrete, Fe and Pb having thicknesses of 3- and 5-mfp for normally incident photons with incident energy of 0.1, 1.0 and 10 MeV. The effects of charged particles depend on the thickness of air following the shield. We use 10 cm air immediately following the shield. It is desirable to calculate for thicker shields than 5 mfp, but we limited the calculations to 5 mfp due to statistical problems. It was determined by Rogers[8] that the absorbed doses for a water phantom were almost the same as those for a soft tissue equivalent phantom in the case of photons.

Figure 2 shows the energy spectrum of photons or charge particles behind water, concrete, Fe and Pb having thickness of 5 mfp for normally-incident photons of incident energy 0.1 MeV, 1 MeV and 10 MeV. The cut-off kinetic energy is set to 10 and 200 keV for photons and charged particles, respectively, for all materials. Fluorescence photons and bremsstrahlung are also included in the EGS4 calculation. The energy spectrum of charged particles is not different with various shielding materials but that of photons has a different shape depending on the shielding material. In the case of lead, fluorescence photons are remarkable at 0.1 and 1 MeV case. Annihilation photons are remarkable at 10 MeV. In the case of a 0.1 MeV source for low Z materials like water or concrete, the low energy portion is larger than for those of other materials due to the effects of multiscattering.

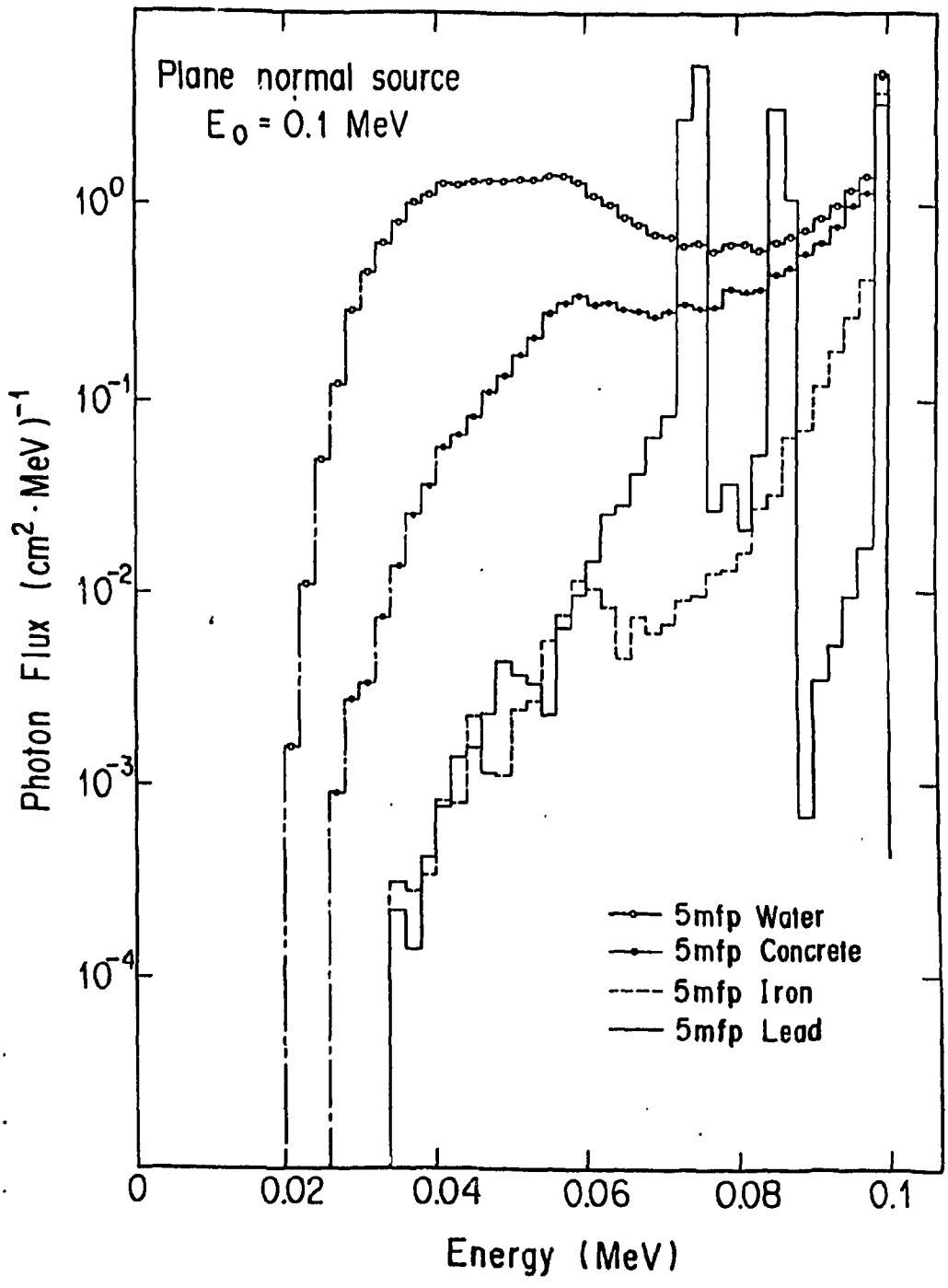

Fig. 2(a) Energy spectrum of photons behind water, concrete, Fe and Pb having a thickness of 5 mfp for normally incident photons with incident energy of 0.1 MeV.

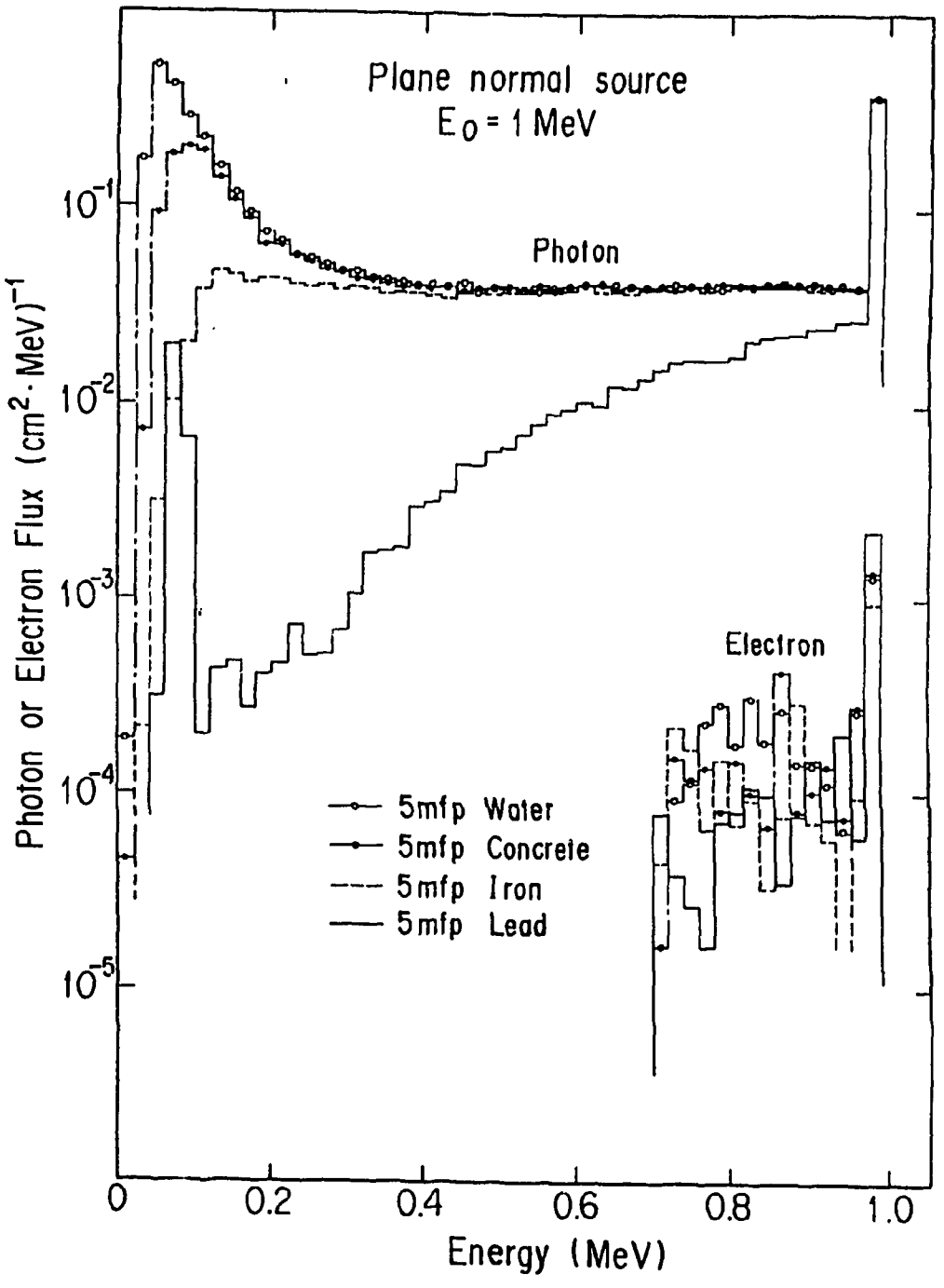

Fig. 2(b) Energy spectrum of photons or charged particles behind water, concrete, Fe and Pb having a thickness of 5 mfp for normally incident photons with incident energy of 1 MeV.

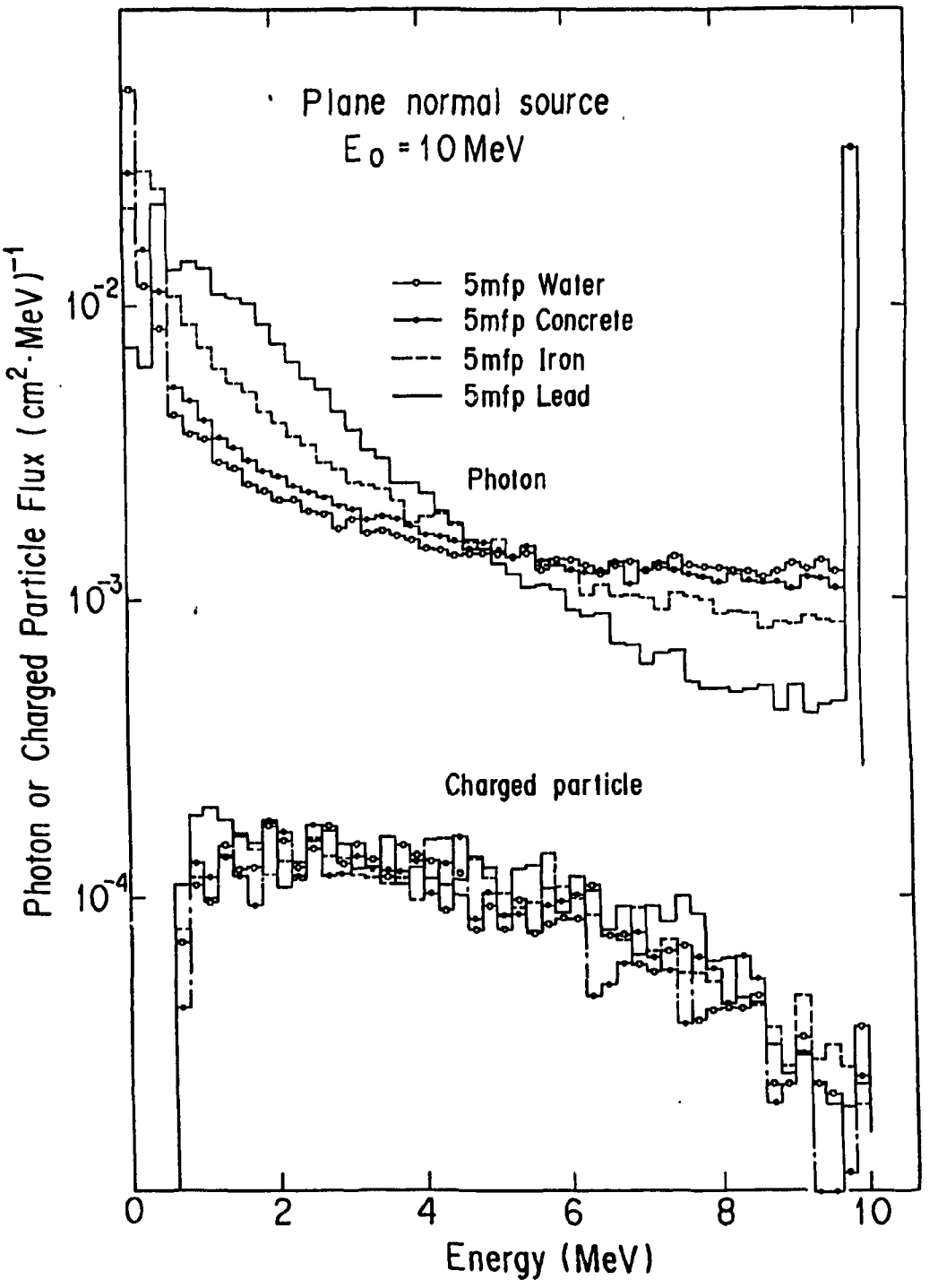

Fig. 2(c) Energy spectrum of photons or charged particles behind water, concrete, Fe and Pb having a thickness of 5 mfp for normally incident photons with incident energy of 10 MeV.

The absorbed energy fraction of incident photons, backscattered photons inside the phantom and incident charged particles at the surface (0 to 0.1 cm from surface) and 1-cm (1 to 1.1 cm from surface) depth of the water phantom behind 5-mfp thick shielding material followed by a 10-cm air region is shown in Table 1. The cut-off kinetic energy of photons is set to 1 and 10 keV and that of charged particles to 10 and 50 keV for air and the water phantom, respectively. Material dependence of the fractions can be seen at the surface due to the difference in the energy spectrum of the incident photons. On the other hand, material dependence becomes smaller at 1-cm depth for the same incident photon energy. This tendency shows that the photon energy spectrum inside the water phantom is similar to that for all other materials due to the scattering inside the phantom in spite of the differences of the incident photon energy spectrum. The contribution of each fraction depends more on the primary photon energy than on the shielding material. The backscattering contribution at 0.1 MeV is larger than that at 1 or 10 MeV and larger at 1 cm depth than at the phantom surface. The charged particle contribution at 1 MeV is between 20 and 40 % at the surface but negligibly small at 1-cm depth due to the short range of charged particles incident on the phantom. At 10 MeV, the charged particle contribution becomes almost 80 % at the surface and is over 30 % even at the 1 cm depth for all materials.

To see this tendency in more detail, the absorbed dose distribution of forward photons, backscatterd photons, forward and backscattered charged particles behind 5-mfp thick shielding material followed by a 10-cm air region for 10 MeV normal incidence is shown in Figure 3. The differences of the contribution at the surface due to the difference in the incident photon spectrum can be seen clearly in this figure. The contribution of charged particles is dominant at the surface but decreases rapidly with increase of depth. It is less than that of the backscattered photons at positions deeper than 3 cm. The contribution of backscattered charged particles is about same as that of backscattered photons, but it also decreases with increase of depth. At depths greater than 1 cm, it becomes negligibly small.

2.3. Comparison of $H(10)$

As mentioned in the introduction, the ambient dose equivalent ,$H^*(10)$, in a complex field such as behind shielding material is generally not equal to $H(10)$. Therefore, it is necessary to know the relation between $H^*(10)$ and $H(10)$ for the application of $H^*(10)$ to shielding calculations. A slab phantom is used for the following calculations. Table 2 shows the ratio of 1-cm dose equivalents $[H(10, photon)]$ calculated from both photon energy fluence and mass energy transfer coefficient , ambient dose equivalent$[H^*(10)]$ and maximum dose equivalent $[H_{max}]$ to 1-cm dose equivalent $[H(10)]$

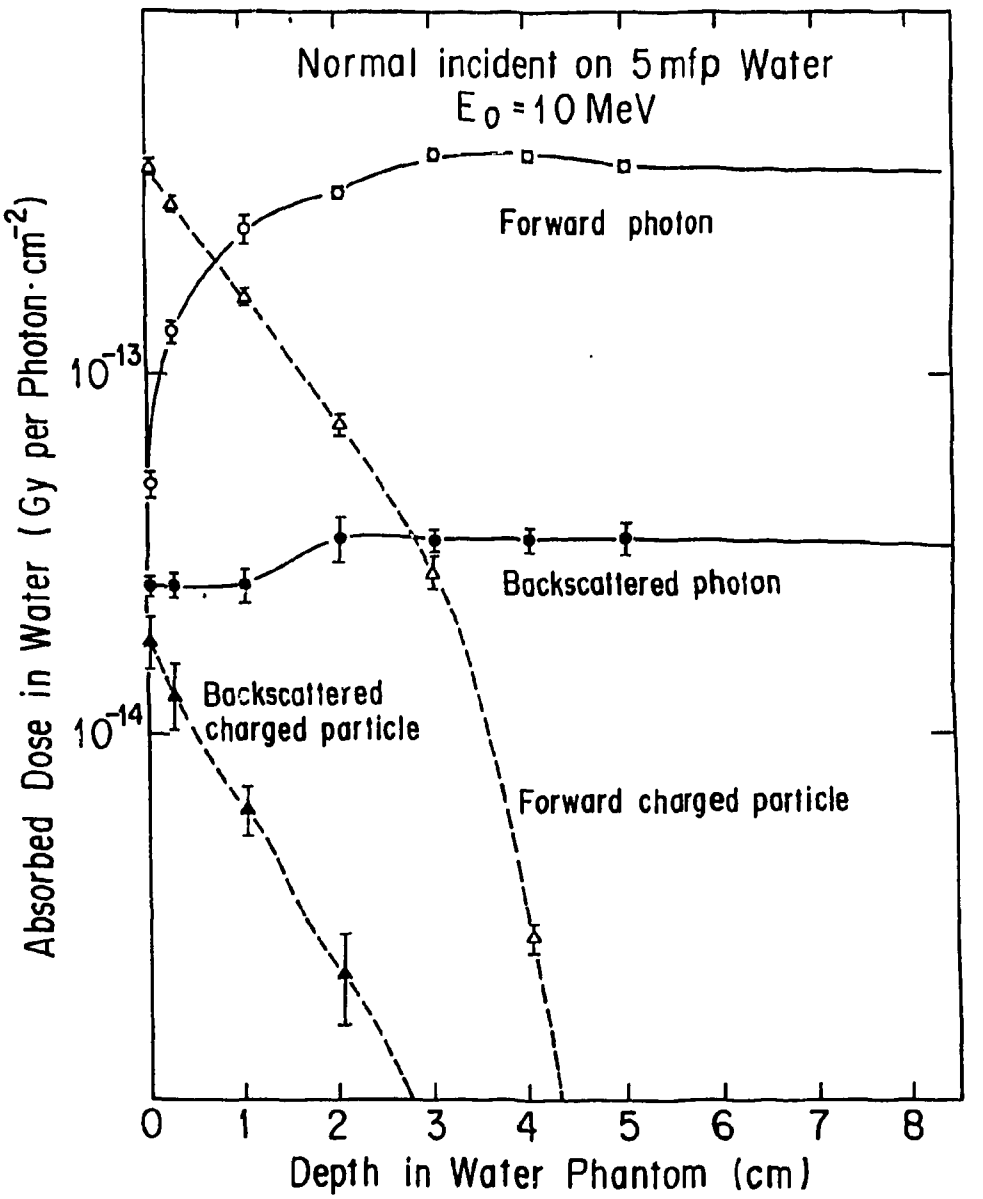

Fig. 3(a) Absorbed dose distribution of forward photons, backscatterd photons, forward and backscattered charged particles behind 5-mfp thick water followed by a 10-cm air region for 10 MeV normal incidence.

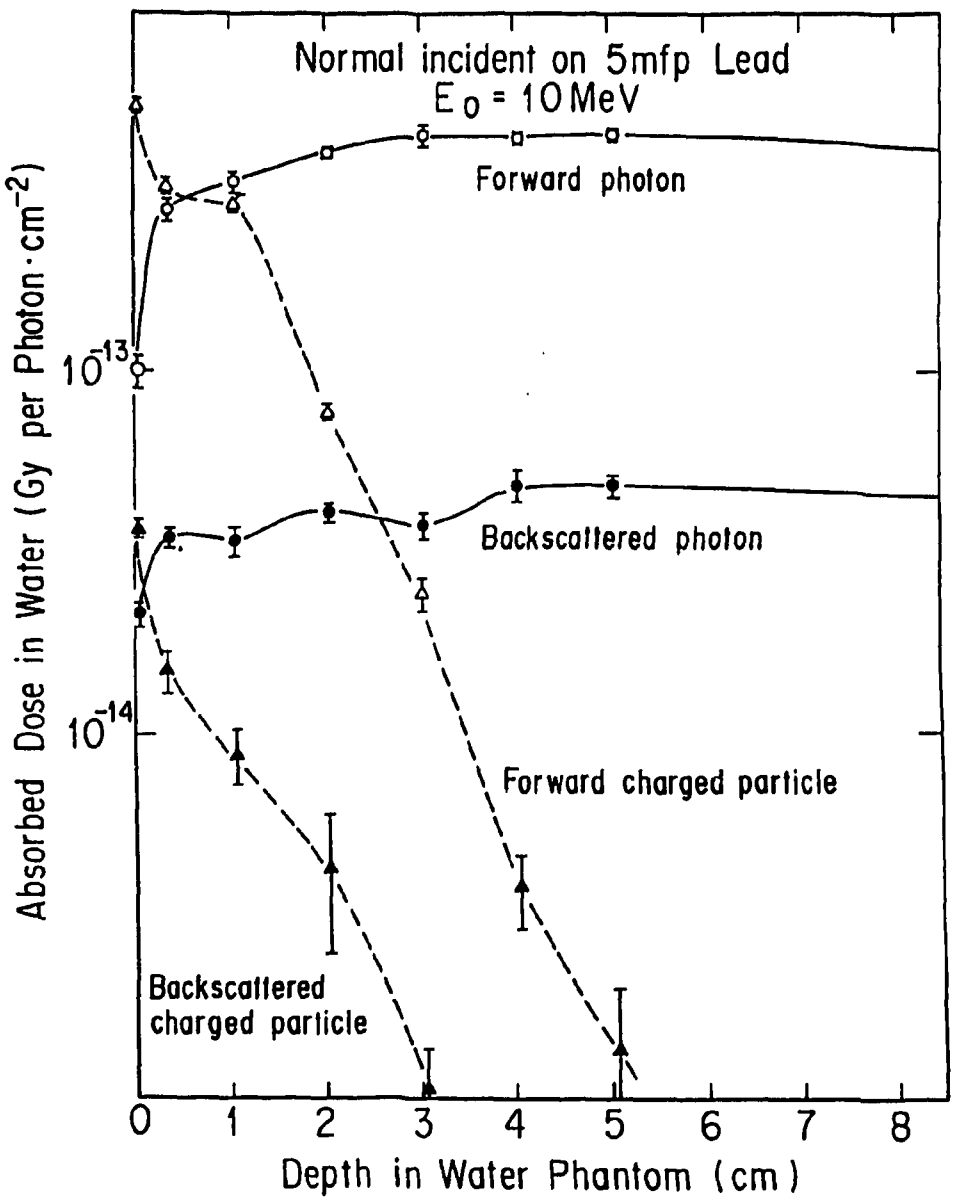

Fig. 3(b) Absorbed dose distribution of forward photons, backscatterd photons, forward and backscattered charged particles behind 5-mfp thick Pb followed by a 10-cm air region for 10 MeV normal incidence.

calculated from energy deposition inside a 30-cm water phantom, which is located behind 3- or 5-mfp thick shielding material followed by a 10-cm air region. $H(10, photon)$ has the tendency to slightly underestimate $H(10)$ in the higher energy region but agrees with $H(10)$ within 10%. On the other hand, $H^*(10)$ agrees with $H(10)$ at 0.1 and 1 MeV but is about a half of $H(10)$ at 10 MeV. This comes from the ignoring of the contribution of secondary charged particles created in air in the Rogers' conversion factor shown in Figure 1 and resulting smaller conversion factor than that of ICRU sphere for higher energy photons. H_{max} is almost same as $H(10, photon)$ at 10 MeV. The 1-cm dose equivalent conversion factor for the ICRU sphere which were adopted by ICRP is almost same as the maximum dose equivalent conversion factor for the slab phantom shown in Figure 1. Therefore, it is supposed that $H^*(10)$ calculated with 1 cm dose equivalent conversion factor can evaluate $H(10)$ within 20 % in the energy region between 0.1 and 10 MeV. It is necessary to pay attention to the sight underesmation tendency in the higher energy region.

3. Application of $H^*(10)$ to Shielding Calculation of Photons

It is very important to know how to include $H^*(10)$ in a practical shielding calculation, especially for photons, because simple equations, such those for point kernel methods, are widely used for shielding calculations. It is possible, of course, to re-evaluate various parameters like exposure buildup factors corresponding to $H^*(10)$, but it would be very big project and not easy to do. It is more practical to modify exposure or absorbed energy in air with a correction factor. This method is useful to compare with the previous data calculated in the form of exposure. In this section, we consider the average conversion factor which converts exposure of finite geometry to $H^*(10)$ and the practical conversion factors which convert exposure obtained with the point kernel method by using point isotropic buildup factors for infinite geometry to $H^*(10)$.

3.1. Average Exposure to 1-cm Dose Equivalent Conversion Factor

Exposure, X (R), and $H^*(10)$ (Sv) behind shielding material of thickness t are given by the following equations.

$$X = \int (X_0(E)/\phi)\phi(E,t)dE, \tag{1}$$

$$H^*(10) = \int (H_0(E)/\phi_{1cm})\phi(E,t)dE, \tag{2}$$

where, $\phi(E,t)$ is the energy spectrum of photons behind a shield of t cm with intial energy E_0, $(X_0(E)/\phi)$ is the conversion factor from unit fluence to exposure, and $(H_0(E)/\phi_{1cm})$ is the conversion factor from unit fluence to 1-cm dose equivalent of ICRU sphere[16]. If we define $f_{1cm}(E)$ as the ratio of $(X_0(E)/\phi)$ to $(H_0(E)/\phi)_{1cm}$, eq. (2) can be expressed as

$$H^*(10) = \int f_{1cm}(E)(X_0(E)/\phi)\phi(E,t)dE. \tag{3}$$

By introducing average exposure to 1-cm dose equivalent conversion factor (average conversion factor) defined by the following equation,

$$\bar{f}_{1cm} = \frac{\int f_{1cm}(E)(X_0(E)/\phi)\phi(E,t)dE}{\int (X_0(E)/\phi)\phi(E,t)dE}, \tag{4}$$

the 1-cm dose equivalent can be expressed with the exposure and average conversion factor as follows.

$$\begin{aligned} H^*(10) &= \bar{f}_{1cm} \int (X_0(E)/\phi)\phi(E,t)dE \\ &= \bar{f}_{1cm} X. \end{aligned} \tag{5}$$

Eq. (5) shows that exposure can be converted to $H^*(10)$ easily if we evaluate the average conversion factor as a function of the exposure geometry, photon energy, shielding material and its thickness. Average conversion factors for each shielding material calculated by EGS4 and PALLAS are shown in Figure 4. Except the case of water at 0.1 MeV, the average exposure to 1-cm dose equivalent conversion factors have a tendency to slightly increase with an increase of the shield thickness but become constant beyond 10 mfp. The average conversion factor of water at 0.1 MeV decreases with an increase of shield thickness. This tendency is due to the drastic decrease of f_{1cm} below 0.06 MeV where the photon flux increases with the scattering inside the material shown in Figure 2(a). In this case also, the average conversion factor is almost constant above 10 mfp. In a practical design, it is possible to evaluate $H^*(10)$ on the safe side by using the maximum average conversion factor for each material, depending only on the energy of the incident photons. Figure 5 shows the maximum average conversion factors calculated with PALLAS between 1 and 30 mfp for water, concrete, Fe

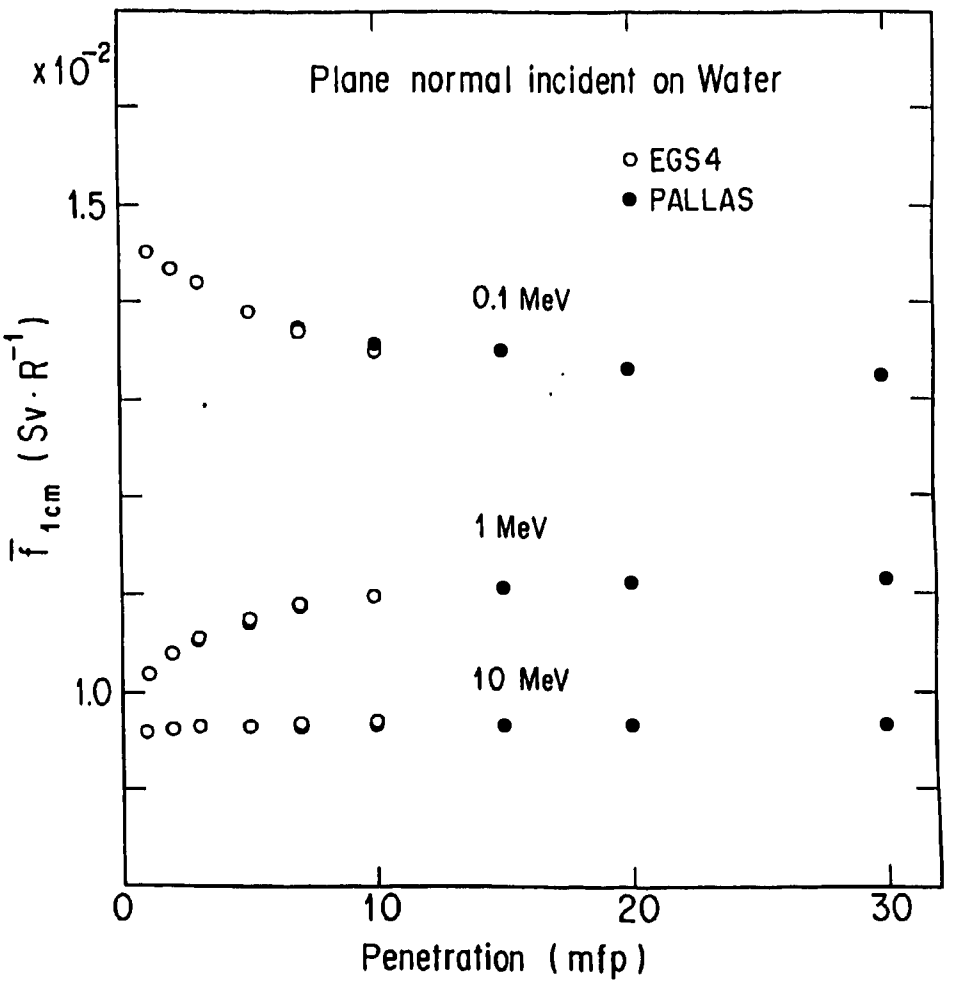

Fig. 4(a) Average exposure to 1-cm dose equivalent conversion factors for water as a function of thickness of slab in mfp.

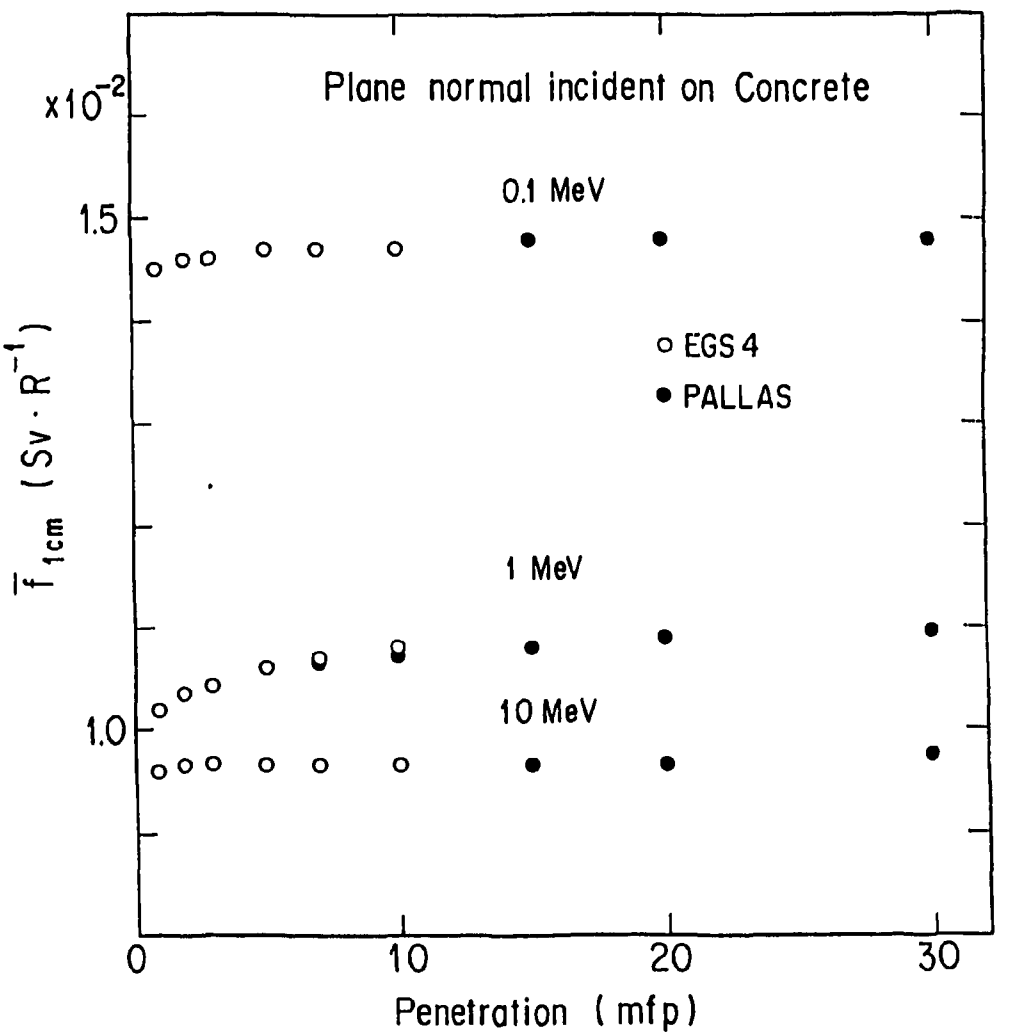

Fig. 4(b) Average exposure to 1-cm dose equivalent conversion factors for concrete as a function of thickness of slab in mfp.

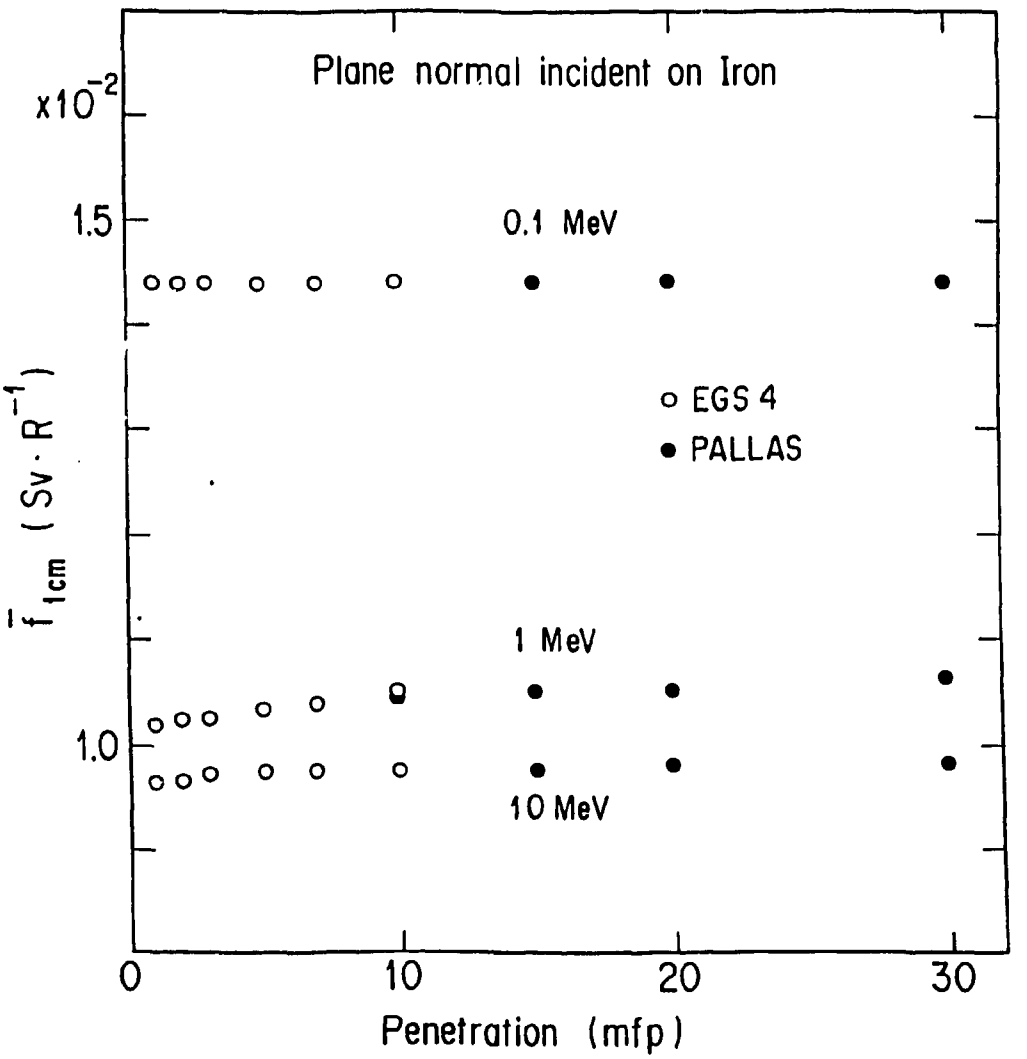

Fig. 4(c) Average exposure to 1-cm dose equivalent conversion factors for Fe as a function of thickness of slab in mfp.

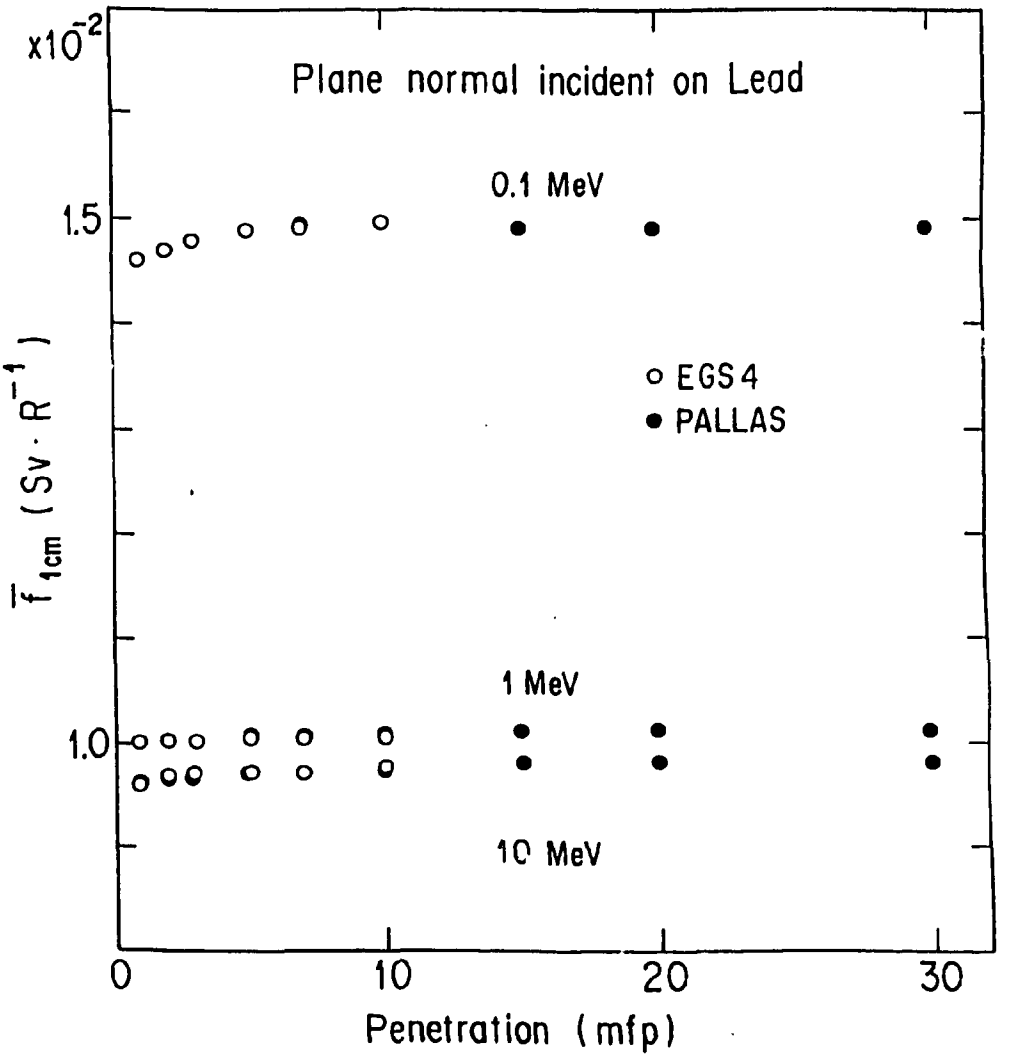

Fig. 4(d) Average exposure to 1-cm dose equivalent conversion factors for Pb as a function of thickness of slab in mfp.

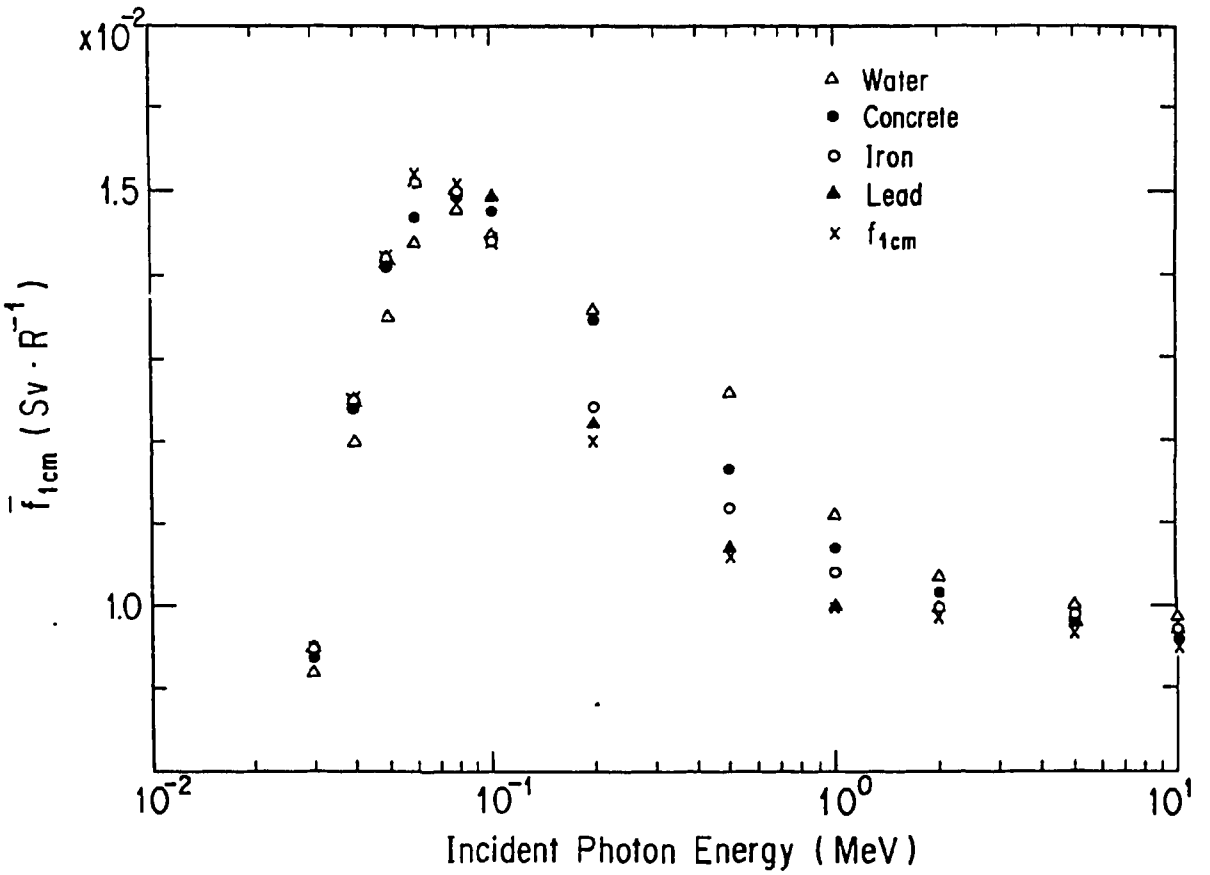

Fig. 5 Maximum average conversion factors between 1 and 30 mfp and exposure to 1 cm dose equivalent conversion factors as a function of incident photon energy.

and Pb together with calculated exposure to 1-cm dose equivalent conversion factors as a function of incident photon energy. The large values of the average conversion factors in the region between 0.06 and 0.1 MeV come from the effects of backscattering inside the phantom. Average conversion factors are smaller than $f_{1cm}(E)$ below 0.08 MeV and larger above 0.08 MeV. This shows that the energy spread due to scattering inside the shield affects the average conversion factor.

3.2. Practical Exposure to 1 cm Dose Equivalent Conversion Factor

If it is possible to get the exposure for a finite thickness by using the attenuation curve for a shielding material, we can convert it to $H^*(10)$ by using the average conversion factor mentioned in the previous section. But the effects of backscattering due to the shielding material must be considered when using the point kernel method based on the finite-medium point isotropic buildup factor. For conversion factors corresponding to this situation, we define the practical exposure to 1-cm dose equivalent conversion factor (practical conversion factor) as follows.

$$\bar{f}_{p,1cm} = \frac{\int f_{1cm}(E)(X_0(E)/\phi)\phi(E,t)dE}{\int (X_0(E)/\phi)\phi_{inf}(E,t)dE}, \tag{6}$$

where, $\phi_{inf}(E,t)$ is the photon energy spectrum at the depth t in the infinite material.

If we evaluate practical conversion factors as a function of the exposure geometry, photon energy, shielding material and its thickness, the exposure for an infinite medium can be converted to $H^*(10)$ by the following equation:

$$\begin{aligned} H^*(10) &= \bar{f}_{p,1cm} \int (X_0(E)/\phi)\phi_{inf}(E,t)dE \\ &= \bar{f}_{p,1cm} X_{inf}, \end{aligned} \tag{7}$$

where, X_{inf} is exposure in an infinite medium.

Practical conversion factors for water and Pb calculated with EGS4 and PALLAS are shown in Figure 6. The practical conversion factors depend more on the thickness of shield than on the average conversion factors in the case of Pb, except for 1 MeV, but are almost constant above 10 mfp like the average conversion factor. This tendency can be seen in the case of concrete and Fe. On the other hand, the practical conversion factors for water have large values at higher energy and decrease with an increase of shield thickness. This is the reverse tendency compared to the average conversion factors and may come from the fact that the increase of 1-cm dose equivalent conversion factor due to backscattering inside the phantom corresponds to the increase of exposure in the infinite medium.

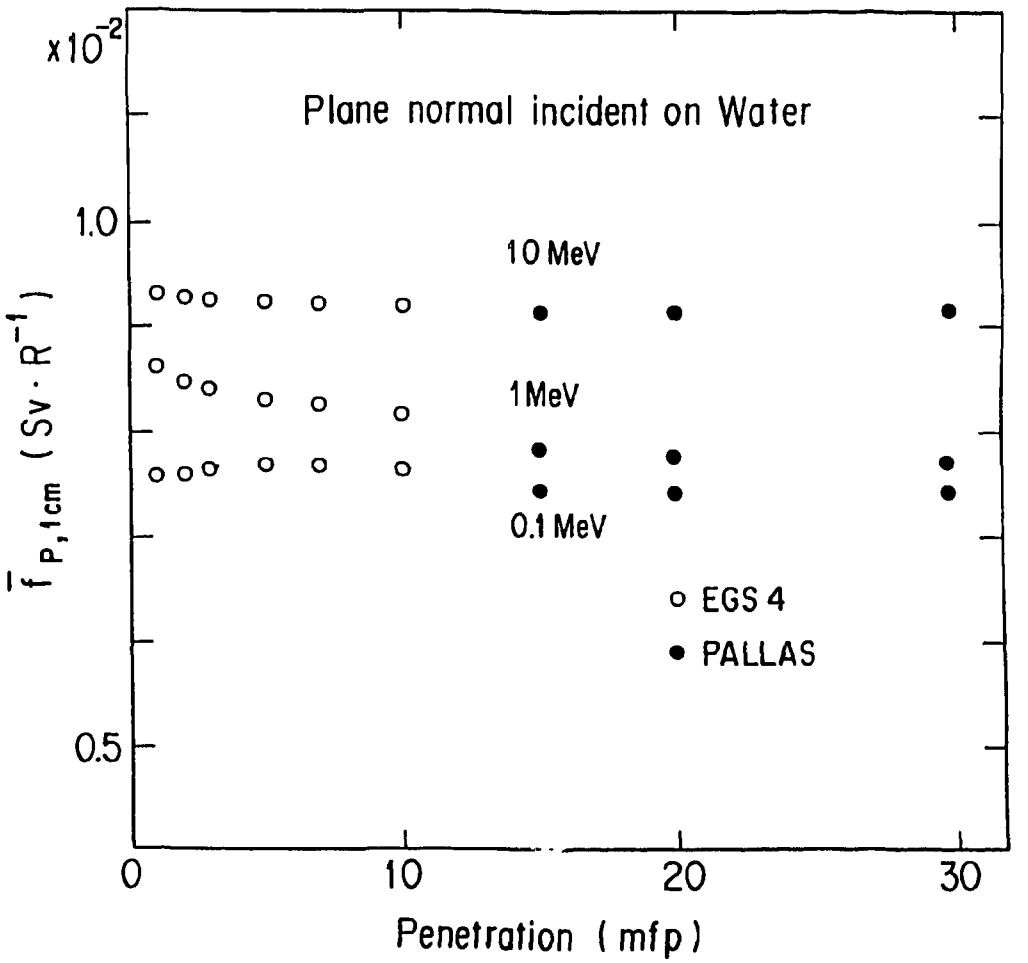

Fig. 6(a) Practical exposure to 1-cm dose equivalent conversion factors of water as a function of slab in mfp.

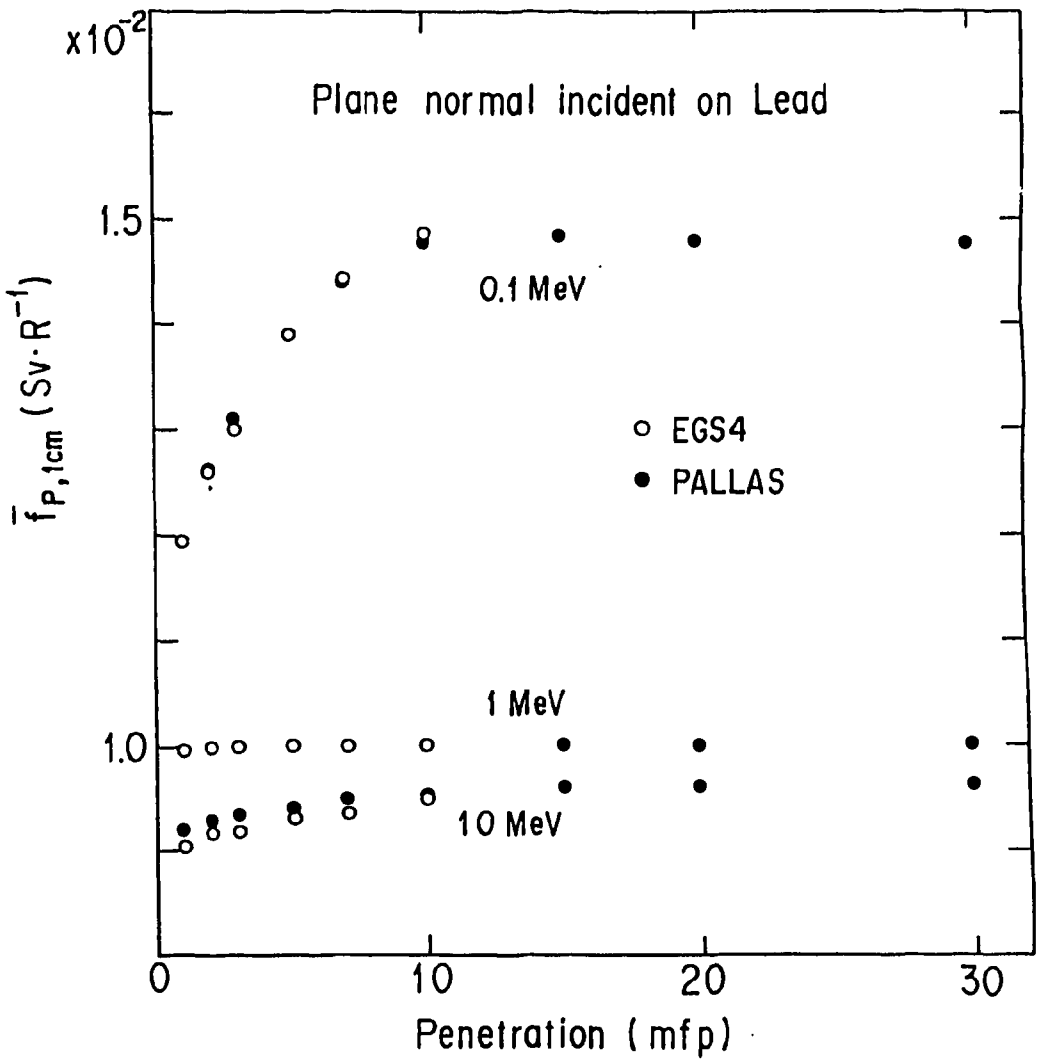

Fig. 6(b) Practical exposure to 1-cm dose equivalent conversion factors of Pb as a function of slab in mfp.

It is possible to evaluate $H^*(10)$ on the safe side by using the maximum practical conversion factor beyond 1 mfp for each material depending only the energy of the incident photons. Figure 7 shows the maximum practical conversion factors calculated with PALLAS between 1 and 30 mfp for water, concrete, Fe and Pb together with exposure to 1 cm dose equivalent conversion factors as a function of incident photon energy. In general, the practical conversion factors are smaller than the average conversion factors due to backscattering inside the medium and this tendency is remarkable for water and concrete. Except near 0.1 MeV, the practical conversion factors of all materials are smaller than $f_{1cm}(E)$.

The contributions of backscattering in an infinite medium are sometimes used as one of the safety factors in point kernel calculations. To keep this idea, the average conversion factor must be used instead of the practical conversion factor.

4. Conclusion

Appropriateness of the ambient dose equivalent used to evaluate the 1-cm dose equivalent which has been adopted in the revised regulation as the effective dose equivalent was investigated behind shielding materials of water, concrete, Fe and Pb. By comparing the absorbed energy in a slab phantom with the 1-cm dose equivalent conversion factor or maximum dose equivalent conversion factor for a slab phantom, it became clear that the ambient dose equivalent calculated with the 1-cm dose equivalent conversion factor can evaluate the 1-cm dose equivalent within 20 % but having a slight underestimating tendency at higher energies. The average 1-cm dose equivalent conversion factors, which convert exposure for an finite medium to ambient dose equivalent and the practical 1-cm dose equivalent conversion factors, which convert exposure for an infinite medium to ambient dose equivalent, were introduced and presented as the recommended way to apply 1-cm dose equivalent to a practical shield calculation. Dependences of both conversion factors on the shielding material, its thickness and incident photon energy were studied. Both conversion factors have constant values above 10 mfp. The maximum values of both conversion factors between 1 and 30 mfp can be used as the conversion factors, only depending on the material and photon energy. The results obtained by using this conversion factor is always larger than $H^*(10)$.

All discussions above apply to a plane parallel beam in plane geometry. It was confirmed that both conversion factors for the point isotropic case are almost same as those for plane geometry from calculations by EGS4 and PALLAS. Effective 1-cm dose equivalent conversion factors, which

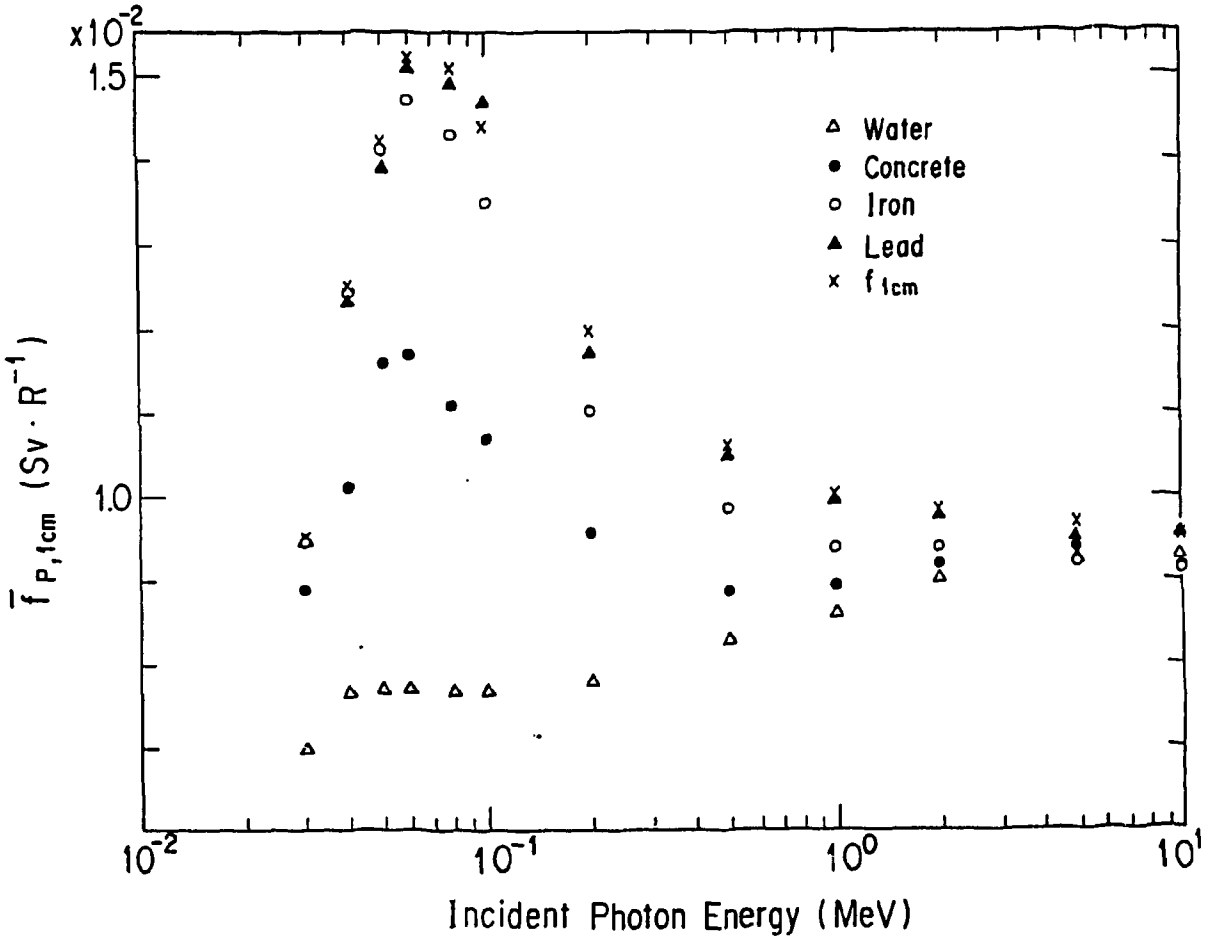

Fig. 7 Maximum practical exposure to 1-cm dose equivalent conversion factor between 1 and 30 mfp and exposure to 1-cm dose equivalent conversion factors as a function of incident photon energy.

convert absorbed dose of air (Gy) to ambient dose equivalent, were proposed by Tanaka et al.[12]. Effective conversion factors are obtained multiplied 115 to average conversion factors. By the same way, practical conversion factors to absorbed dose of air are given by multiplied 115 to practical conversion factors.

Gopinath and Subbaiah calculated correction factors of buildup factors[13] to include the effects of a phantom behind a shield. Their correction factors cannot be compared directly with above conversion factors but it is necesary to study relations between correction factors and conversion factors.

There are various opinions concerning the use of 1-cm dose equivalent or ambient dose equivalent, and 1-cm dose equivalent has not been adopted by all countries. Some have the opinion that the ICRU-defined effective dose equivalent should be used for evaluating the conversion factors[14]. In this study, we performed various investigations from the view points of using 1-cm dose equivalent and ambient dose equivalent. But it is necessary to discuss these problems within the wide fields of scientists before a consensus can be reached.

Acknowledgements: The authors would like to thank K. Katoh and S. Ban at KEK, National Laboratory for High Energy Physics, for their valuable discussions. The authors also wish to show their sincere thanks to D. K. Trubey for his great assistance in publishing the translated report.

REFERENCES

1. T. Yamaguch, J. the Atomic Energy Society of Japan, 30, 754 (1988).
2. T. Hamada, M. Takashi and J. Akaishi, ibid. 30, 876 (1988).
3. W. R. Nelson, H. Hirayama and D. W. O. Rogers, "EGS4 code system", SLAC-265, Stanford Linear Accelerator (1985).
4. K. Takeuchi and S. Tanaka, "PALLAS-1D(VII); A code for direct integration of transport equation in one dimensional plane and spherical geometries, JAERI-M-84-214 (1984).
5. D. W. O. Rogers, Health Phys., 46, 891 (1984).
6. G. Williams, et al., "Calculation and analysis of photon dose equivalent distributions in the ICRU sphere", GSF Bericht S-958 (1983).
7. P. J. Dimbylow and T. M. Francis, Radat. Prot. Dosim., 9, 49 (1984).
8. P. J. Dimbylow and T. M. Francis, Phys. Med. Biol., 28, 817 (1983).
9. P. J. Dimbylow and T. M. Francis, Phys. Med. Biol., 28, 817 (1983).
10. Edited by T. Maruyama, "Manual of Measurement and Estimation of Dose Equivalent for External Exposure",Technical Center for Safety of Atomic Energy, (1988).
11. S. Tanaka and T. Suzuki, Radioisotopes, 38, 90 (1989).
12. D. V. Gopinath and K. V. Sabbaiah, Nucl. Sci. Eng., 97, 362-373 (1987).
13. D. C. Kaul, "Fluence-to-dose conversion factor standards", Trans. Am. Nucl. Soc., 57, 214 (1988).

Table 1 Absorbed energy fraction at a surface and a 1 cm depth of water phantom behinde a 5-mfp thick shielding material followed with a 10 cm air region.

Material	Position	Photon energy	Absorbed energy fraction		
			Forward photons	Backscattered photons	Charged particles
Water	Surface (0-0.1cm)	0.1 MeV	0.55±0.03	0.42±0.03	0.03±0.01
		1.0 MeV	0.55±0.03	0.23±0.02	0.22±0.02
		10.0 MeV	0.11±0.01	0.06±0.004	0.83±0.04
	1 cm (1-1.1cm)	0.1 MeV	0.56±0.03	0.44±0.02	------
		1.0 MeV	0.79±0.04	0.21±0.01	------
		10.0 MeV	0.55±0.06	0.06±0.01	0.39±0.03
Concrete	Surface (0-0.1cm)	0.1 MeV	0.56±0.03	0.39±0.02	0.05±0.01
		1.0 MeV	0.57±0.04	0.19±0.01	0.24±0.02
		10.0 MeV	0.12±0.02	0.05±0.004	0.83±0.02
	1 cm (1-1.1cm)	0.1 MeV	0.59±0.03	0.41±0.03	------
		1.0 MeV	0.81±0.04	0.19±0.01	------
		10.0 MeV	0.55±0.03	0.06±0.01	0.39±0.02
Iron	Surface (0-0.1cm)	0.1 MeV	0.62±0.04	0.33±0.02	0.05±0.02
		1.0 MeV	0.64±0.06	0.16±0.01	0.20±0.03
		10.0 MeV	0.15±0.01	0.04±0.003	0.81±0.04
	1 cm (1-1.1cm)	0.1 MeV	0.58±0.04	0.42±0.03	------
		1.0 MeV	0.81±0.04	0.19±0.01	------
		10.0 MeV	0.58±0.02	0.06±0.01	0.36±0.01
Lead	Surface (0-0.1cm)	0.1 MeV	0.67±0.05	0.31±0.03	0.02±0.01
		1.0 MeV	0.43±0.03	0.11±0.01	0.46±0.04
		10.0 MeV	0.14±0.02	0.03±0.002	0.82±0.03
	1 cm (1-1.1cm)	0.1 MeV	0.58±0.04	0.42±0.04	------
		1.0 MeV	0.86±0.08	0.14±0.02	------
		10.0 MeV	0.58±0.03	0.06±0.01	0.36±0.02

Table 2 Ratio of a 1-cm dose equivalent calculated from both photon energy fluence and mass energy transfer coefficient, ambient dose equivalent and a maximum dose equivalent to a 1-cm dose equivalent calculated from energy deposition inside a 30-cm water phantom, which is located behinde a 3- or 5-mfp thick shielding material followed with a 10-cm air region.

Material	Photon energy	Shield thickness	H(10, photon)/H(10)	H*(10)/H(10)	H_{max}/H(10)
Water	0.1 MeV	3 mfp	1.05±0.02	1.06±0.02	1.08±0.02
		5 mfp	1.05±0.04	1.07±0.03	1.09±0.03
	1.0 MeV	3 mfp	1.05±0.01	1.07±0.02	1.07±0.02
		5 mfp	1.01±0.03	1.02±0.03	1.03±0.04
	10.0 MeV	3 mfp	0.96±0.01	0.51±0.01	0.94±0.01
		5 mfp	0.99±0.05	0.54±0.03	0.96±0.05
Concrete	0.1 MeV	3 mfp	1.06±0.02	1.11±0.02	1.13±0.02
		5 mfp	1.03±0.04	1.09±0.04	1.11±0.04
	1.0 MeV	3 mfp	0.97±0.01	1.00±0.02	1.00±0.02
		5 mfp	1.00±0.03	1.08±0.03	1.08±0.03
	10.0 MeV	3 mfp	0.93±0.01	0.50±0.01	0.91±0.01
		5 mfp	1.02±0.04	0.58±0.03	1.00±0.04
Iron	0.1 MeV	3 mfp	1.02±0.03	1.01±0.03	1.03±0.03
		5 mfp	1.08±0.05	1.08±0.05	1.10±0.05
	1.0 MeV	3 mfp	1.06±0.03	1.09±0.03	1.09±0.03
		5 mfp	1.06±0.04	1.10±0.04	1.10±0.03
	10.0 MeV	3 mfp	0.89±0.02	0.54±0.01	0.89±0.02
		5 mfp	0.91±0.03	0.59±0.02	0.90±0.03
Lead	0.1 MeV	3 mfp	1.03±0.03	1.17±0.03	1.19±0.03
		5 mfp	1.08±0.05	1.17±0.05	1.19±0.06
	1.0 MeV	3 mfp	1.00±0.03	1.00±0.02	1.00±0.02
		5 mfp	1.00±0.07	1.00±0.07	1.00±0.07
	10.0 MeV	3 mfp	0.90±0.02	0.57±0.01	0.89±0.02
		5 mfp	0.95±0.02	0.68±0.02	0.95±0.02

H(10, photon): 1cm dose equivalent calculated from photon energy fluence and mass energy transfer coefficient
H*(10) : ambient dose equivalent
H_{max} : maximum dose equivalent obtained by using photon fluence to maximum dose equivalent conversion factor
H(10) : 1cm dose equivalent calculated from energy deposition inside a water phantom